Formation of $PPh_2C_6F_5$ through Phosphido Platinum and/or Palladium(III) Intermediates[||,⊥]

Irene Ara,[†] Naima Chaouche,[†,‡] Juan Forniés,*[,†] Consuelo Fortuño,[†] Abdelaziz Kribii,[‡] and Athanassios C. Tsipis*[,§]

Departamento de Química Inorgánica and Instituto de Ciencia de Materiales de Aragón, Universidad de Zaragoza-CSIC, 50009 Zaragoza, Spain, Département de Chimie, Faculté des Sciences, Université IbnTofail, B. P. 133, Kenitra, Morocco, and Laboratory of Inorganic Chemistry, Department of Chemistry, University of Ioannina, 451 10 Ioannina, Greece.

Received September 16, 2005

The two-electron oxidation reactions of the neutral $[(C_6F_5)_2M(\mu\text{-}PR_2)_2M'(NCCH_3)_2]$ (M = M′ = Pt or Pd, M = Pt, M′ = Pd) complexes using I_2 as oxidant have been investigated by experimental (R = Ph) and electronic structure calculation methods (R = H). It was found that a reductive coupling of PR_2 and C_6F_5 takes place along the reaction pathway for all oxidized complexes. The most salient structural features of the $[(C_6F_5)_2Pt(\mu\text{-}PR_2)_2Pd(C_6F_5)_2]^{2-}$, $[(C_6F_5)_2Pd(\mu\text{-}PR_2)_2Pd(acac)]^-$, and $[(C_6F_5)_2Pt(\mu\text{-}PR_2)_2PtI_2]$ complexes (experimental R = Ph) are reproduced very well by the B3LYP/lanl2dz calculations (R = H).

Introduction

The stability and flexibility of the M−P bonds in polynuclear phosphido metal complexes have allowed the synthesis of a rich variety of complexes with peculiar coordination modes of the phosphido ligands.[1−15]

Oxidation of some of these polynuclear complexes resulted in the formation of stable complexes, with all or some of the metal centers in higher formal oxidation state.[16,17] However in some cases, the oxidation process is not the final step of the process and other reactions follow. Thus, we have reported recently that the addition of I_2 to $[NBu_4]_2[(C_6F_5)_2M(\mu\text{-}PPh_2)_2M'(C_6F_5)_2]$ (M, M′ = Pt, Pd) yields at low temperature the dinuclear platinum(III) derivative $[(C_6F_5)_2Pt(\mu\text{-}PPh_2)_2Pt(C_6F_5)_2]$, while $[NBu_4]_2[(C_6F_5)_2M(\mu\text{-}PPh_2)_2M'(C_6F_5)_2]$ (M = Pt, M′ = Pd; M = M′ = Pd) do not afford, under similar conditions, the expected M(III)−M′(III) compounds but the dinuclear M(II)−M′(II) derivatives $[NBu_4][(C_6F_5)_2M(\mu\text{-}PPh_2)(\mu\text{-}I)M'(C_6F_5)(PPh_2C_6F_5)]$ (M, M′ = Pt, Pd) through a process that includes oxidation to the M(III)−M′(III) derivatives followed by a reductive coupling between a C_6F_5 group and a PPh_2 ligand to form the M(II)−M′(II) complexes containing $PPh_2C_6F_5$.[18]

To get a better understanding of the reasons why in this type of complexes the oxidation can be followed by an intramolecular reductive elimination, we have now studied the behavior of the neutral $[(C_6F_5)_2M(\mu\text{-}PPh_2)_2M'(NCCH_3)_2]$ (M = M′ = Pt, **1**; M = Pt, M′ = Pd, **2**; M = M′ = Pd, **3**) derivatives toward I_2. In this process, oxidation/substitution reactions and intramolecular reductive elimination occur and the energetic and electronic profile of the 2e oxidation/reduction of the neutral $[(C_6F_5)_2M(\mu\text{-}PH_2)_2M'(NCCH_3)_2]$ (M = M′ = Pt or Pd, M = Pt, M′ = Pd) complexes has been investigated at the B3LYP/lanl2dz level.

Results and Discussion

Synthesis of $[(C_6F_5)_2M(\mu\text{-}PPh_2)_2M'(NCCH_3)_2]$ (M = Pt, M′ = Pd, 2; M = M′ = Pd, 3). The reaction of $[NBu_4]_2[(C_6F_5)_2Pt(\mu\text{-}PPh_2)_2Pd(C_6F_5)_2]$[19] with $HClO_4$ (1:2 molar ratio, MeOH solution) in CH_3CN results in the selective breaking of the two Pd−C bonds, affording C_6F_5H and $[(C_6F_5)_2Pt(\mu\text{-}PPh_2)_2Pd(NCCH_3)_2]$, **2**. Complex **3** is prepared by reaction of $[NBu_4][(C_6F_5)_2Pd(\mu\text{-}PPh_2)_2Pd(acac)]$[20] with $HClO_4$ (1:1 molar ratio, MeOH solution) in CH_3CN. The protonation of the acetylac-

|| Polynuclear Homo- or Heterometallic Palladium(II)−Platinum(II) Pentafluorophenyl Complexes Containing Bridging Diphenylphosphido Ligands. 20. For part 19 see ref 66.

⊥ Dedicated to Prof. Victor Riera on the occasion of his 70th birthday.

* Corresponding authors. E-mail: (J.F.) juan.fornies@unizar.es; (A.C.T., for comments concerning the theoretical calculations) attsipis@cc.uoi.gr.

† Universidad de Zaragoza-CSIC.

‡ Université IbnTofail.

§ University of Ioannina.

(1) Frenzel, C.; Somoza, F. J.; Blaurock, S.; Hey-Hawkins, E. *Dalton Trans.* **2001**, 3115−3118.

(2) Forniés, J.; Fortuño, C.; Ibáñez, S.; Martín, A.; Tsipis, A. C.; Tsipis, C. A. *Angew. Chem., Int. Ed.* **2005**, *44*, 2407−2410.

(3) Alonso, E.; Forniés, J.; Fortuño, C.; Martín, A.; Orpen, A. G. *Organometallics* **2003**, *22*, 2723−2728.

(4) Falvello, L. R.; Forniés, J.; Fortuño, C.; Durán, F.; Martín, A. *Organometallics* **2002**, *21*, 2226−2234.

(5) Alonso, E.; Forniés, J.; Fortuño, C.; Martín, A.; Orpen, A. G. *Organometallics* **2000**, *19*, 2690−2697.

(6) Alonso, E.; Forniés, J.; Fortuño, C.; Martín, A.; Orpen, A. G. *Chem. Commun.* **1996**, 231−232.

(7) Alonso, E.; Forniés, J.; Fortuño, C.; Tomás, M. *J. Chem. Soc., Dalton Trans.* **1995**, 3777−3784.

(8) Falvello, L. R.; Forniés, J.; Fortuño, C.; Martínez, F. *Inorg. Chem.* **1994**, *33*, 6242−6246.

(9) Mizuta, T.; Onishi, M.; Nakazono, T.; Nakazawa, H.; Miyoshi, K. *Organometallics* **2002**, *21*, 717−726.

(10) Leoni, P.; Vichi, E.; Lencioni, S.; Pasquali, M.; Chiarentin, E.; Albinati, A. *Organometallics* **2000**, *19*, 3062−3068.

(11) Leoni, P.; Marchetti, F.; Pasquali, M.; Marchetti, L.; Albinati, A. *Organometallics* **2002**, *21*, 2167−2182.

(12) Archambault, C.; Bender, R.; Braunstein, P.; Dusausoy, Y. *J. Chem. Soc., Dalton Trans.* **2002**, 4084−4090.

(13) Bender, R.; Braunstein, P.; Bouaoud, S. E.; Rouag, D.; Harvey, P. D.; Golhen, S.; Ouahab, L. *Inorg. Chem.* **2002**, *41*, 1739−1746.

(14) Itazaki, M.; Nishihara, Y.; Osakada, K. *Organometallics* **2004**, *23*, 1610−1621.

(15) Heyn, R. H.; Gorbitz, C. H. *Organometallics* **2002**, *21*, 2781−2784.

(16) Alonso, E.; Casas, J. M.; Cotton, F. A.; Feng, X. J.; Forniés, J.; Fortuño, C.; Tomás, M. *Inorg. Chem.* **1999**, *38*, 5034−5040.

(17) Alonso, E.; Casas, J. M.; Forniés, J.; Fortuño, C.; Martín, A.; Orpen, A. G.; Tsipis, C. A.; Tsipis, A. C. *Organometallics* **2001**, *20*, 5571−5582.

(18) Chaouche, N.; Forniés, J.; Fortuño, C.; Kribii, A.; Martín, A.; Karipidis, P.; Tsipis, A. C.; Tsipis, C. A. *Organometallics* **2004**, *23*, 1797−1810.

(19) Forniés, J.; Fortuño, C.; Navarro, R.; Martínez, F.; Welch, A. J. *J. Organomet. Chem.* **1990**, *394*, 643−658.

10.1021/om0508029 CCC: $33.50
Publication on Web 02/01/2006

Scheme 1

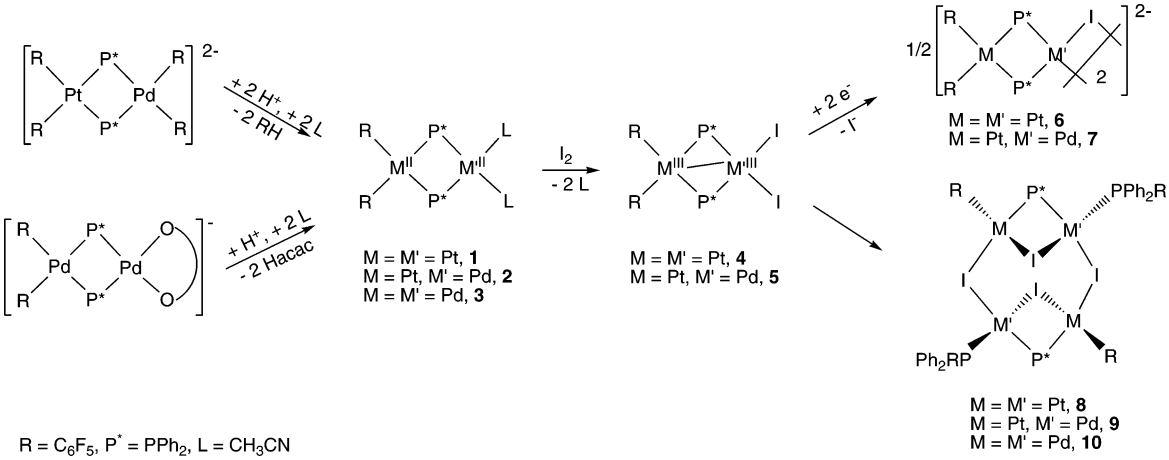

etonate ligand yields Hacac and coordination of two acetonitrile groups. The synthetic procedures for these single complexes imply straightforward coordination chemistry strategies, the phosphido ligands maintaining the polynuclear fragment (see Scheme 1).

Complexes **2** and **3** have been characterized by elemental analysis and IR and NMR spectroscopy. All data are given in the Experimental Section and are in agreement with a structure for **2** and **3** similar to that established for compound **1** (M = M′ = Pt) by X-ray diffraction.[21]

Reactions between $[(C_6F_5)_2M(\mu\text{-}PPh_2)_2M'(NCCH_3)_2]$ and I_2. The reactions of white or yellow suspensions of $[(C_6F_5)_2Pt(\mu\text{-}PPh_2)_2M(NCCH_3)_2]$ (M = Pt, **1**; Pd, **2**) in CH_2Cl_2/CH_3CN or CH_2Cl_2, respectively, with a CH_2Cl_2 solution of I_2 (1:1 molar ratio) at low temperature yield (Scheme 1) the dinuclear derivatives $[(C_6F_5)_2Pt(\mu\text{-}PPh_2)_2MI_2]$ (M = Pt, **4**; Pd, **5**), with the metal centers in a formal oxidation state of III. Nevertheless all attempts to isolate the homodinuclear derivative of palladium(III) $[(C_6F_5)_2Pd(\mu\text{-}PPh_2)_2PdI_2]$ by reacting **3** with I_2 (1:1 molar ratio) at 195 K, even for a very short reaction time, have been unsuccessful. The palladium(III) complex, if obtained, evolves very fast to a very insoluble material, the nature of which will be discussed later.

The crystal structure of complex **4**·$2CHCl_3$ has been determined by X-ray diffraction, and it is shown in Figure 1. Selected bond distances and angles are listed in Table 1.

Complex **4** is a dinuclear compound involving two platinum atoms bridged by diphenylphosphido ligands, with the $Pt(\mu\text{-}PPh_2)_2Pt$ core nearly planar. Both platinum atoms are located in square-planar environments, with the best least-squares planes forming a dihedral angle of 9.3°. The Pt−C, Pt−P, and Pt−I distances are as expected and comparable to distances found in other complexes having the same ligands.[16,17,22−25] The short Pt(1)−Pt(2) distance (2.710(1) Å) is in agreement with a metal−metal bond as expected for a dinuclear complex with 30 valence electron count. The Pt−P−Pt angles are small (73.46° and 73.49°), and the P−Pt−P angles are large (105.50° and 106.24°). This situation is responsible for the distortion in the angles around the platinum atoms in their respective environments. Finally, the C_6F_5 rings are planar and nearly perpendicular to the respective coordination planes of the metal centers to which they are bonded [88.0° Pt(1) and 83.6° Pt(2)].

Crystals of the heteronuclear **5** have been obtained at low temperature, and although the resolution of the structure by X-ray diffraction could not be completed (R = 0.12), the connectivity of the atoms has been established to be analogous to that of complex **4**.

The IR spectra of **4** and **5** are almost superimposable. Two absorptions in the 800 cm^{-1} region are observed in both cases, in agreement with the presence of the cis "$(C_6F_5)_2Pt$" fragment.[26,27] The absorption of the C_6F_5 group in the 950 cm^{-1} region provides information on the oxidation state of the metal center bonded to the C_6F_5 groups. A wavenumber increase of this absorption is observed by increasing the oxidation state of the platinum or palladium center.[16,20,26,28] In the starting materials **1** and **2** the absorption appears in both cases at 953 cm^{-1}, while for the oxidized **4** and **5** these appear at 962 and 964 cm^{-1}, respectively, in keeping with the oxidation process. The ^{19}F NMR spectra of **4** and **5** in $CDCl_3$ show three signals in 2:1:2 intensity ratio due to the *o*-F, *p*-F, and *m*-F atoms, respectively, and platinum satellites are observed in the *o*-F signal. This pattern indicates that both C_6F_5 groups are equivalent and that within each ring the two *o*-F atoms are equivalent, as are the *m*-F atoms as well. This is in agreement with the planarity of the molecule observed in the solid state. The spectrum of complex **5** has been recorded at low temperature to avoid evolution of the product (see below). The ^{31}P NMR spectra of **4** and **5** in $CDCl_3$ show a very low field signal with platinum satellites, from which the values of $^1J_{Pt,P}$ can be calculated (see Experimental Section).

The reaction process that yields **4** and **5** is formally the oxidation of the M(II) derivatives by I_2 and substitution of the acetonitrile by the I^- formed. Thus in both complexes the metal centers display a formal oxidation state of III, and the total valence electron count of 30 requires the presence of a metal−metal bond. In agreement with this, the intermetallic distance in **4** is short (2.710(1) Å), and the chemical shifts of the P atoms

(20) Alonso, E.; Forniés, J.; Fortuño, C.; Martín, A.; Orpen, A. G. *Organometallics* **2003**, *22*, 5011−5019.
(21) Ara, I.; Chaouche, N.; Forniés, J.; Fortuño, C.; Kribii, A.; Martín, A. *Eur. J. Inorg. Chem.* **2005**, 3894−3901.
(22) Bellitto, C.; Bonamico, M.; Dessy, G.; Fares, V.; Flamini, A. *J. Chem. Soc., Dalton Trans.* **1986**, 595−601.
(23) Mitsumi, M.; Murase, T.; Kishida, H.; Yoshinari, T.; Ozawa, T. Y.; Toriumi, K.; Sonoyama, T.; Kitagawa, H.; Mitani, T. *J. Am. Chem. Soc.* **2001**, *123*, 11179−11192.
(24) Terheijden, J.; van Koten, G.; van Beek, J. A. M.; Vriesema, B. K.; Kellogg, R. M.; Zoutberg, M. C.; Stam, C. H. *Organometallics* **1987**, *6*, 89−93.
(25) Landis, C. R.; Sawyer, R. A.; Somsook, E. *Organometallics* **2000**, *19*, 994−1002.
(26) Usón, R.; Forniés, J. *Adv. Organomet. Chem.* **1988**, *28*, 219−297.
(27) Maslowsky, E. J. *Vibrational Spectra of Organometallic Compounds*; Wiley: New York, 1977.
(28) Alonso, E.; Forniés, J.; Fortuño, C.; Martín, A.; Orpen, A. G. *Organometallics* **2001**, *20*, 850−859.

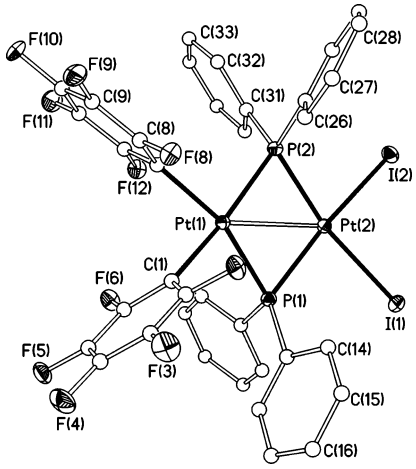

Figure 1. Structure of complex $[(C_6F_5)_2Pt(\mu\text{-}PPh_2)_2PtI_2]$ (**4**).

Table 1. Bond Lengths (Å) and Angles (deg) for $[(C_6F_5)_2Pt(\mu\text{-}PPh_2)_2PtI_2]\cdot 2CHCl_3$

Pt(1)−C(7)	2.065(4)
Pt(1)−C(1)	2.086(4)
Pt(1)−P(1)	2.2542(12)
Pt(1)−P(2)	2.2772(12)
Pt(1)−Pt(2)	2.7101(4)
Pt(2)−P(2)	2.2547(12)
Pt(2)−P(1)	2.2548(12)
Pt(2)−I(2)	2.6334(4)
Pt(2)−I(1)	2.6437(4)
C(7)−Pt(1)−C(1)	84.86(17)
C(7)−Pt(1)−P(1)	161.20(12)
C(1)−Pt(1)−P(1)	85.15(12)
C(7)−Pt(1)−P(2)	87.52(12)
C(1)−Pt(1)−P(2)	165.11(12)
P(1)−Pt(1)−P(2)	105.50(4)
P(2)−Pt(2)−P(1)	106.24(4)
P(2)−Pt(2)−I(2)	81.99(3)
P(1)−Pt(2)−I(2)	168.37(3)
P(2)−Pt(2)−I(1)	169.46(3)
P(1)−Pt(2)−I(1)	83.00(3)
I(2)−Pt(2)−I(1)	89.651(14)

in the NMR spectra of both complexes appear at very low field. These structural data are similar to the ones observed in the diplatinum(III) derivative $[(C_6F_5)_2Pt(\mu\text{-}PPh_2)_2Pt(C_6F_5)_2]$ reported previously.[16]

The oxidation of the acetonitrile derivatives **1** and **2** with I_2 deserves some comments by comparing with the oxidation of the pentafluorophenyl complexes. Treatment of the anions $[(C_6F_5)_2M(\mu\text{-}PPh_2)_2M'(C_6F_5)_2]^{2-}$ with I_2 allows only the isolation of the neutral diplatinum(III) intermediate $[(C_6F_5)_2Pt(\mu\text{-}PPh_2)_2Pt(C_6F_5)_2]$ since the palladium-containing complexes (PtPd, Pd_2) can be neither isolated nor detected, and the binuclear complexes $[NBu_4][(C_6F_5)_2M(\mu\text{-}PPh_2)(\mu\text{-I})M'(C_6F_5)(PPh_2C_6F_5)]$ (M, M′ = Pt, Pd)[18] are obtained instead as a result of the intramolecular PPh_2/C_6F_5 reductive coupling. The reactions described here allow the isolation of not only the dinuclear platinum(III) **4** but also the heterodinuclear derivative **5**.

It has to be noted that dinuclear platinum(III) complexes[29,30] are well known today, while only one dinuclear palladium(III) derivative has been reported so far.[31,32] Usually, these derivatives display the metal centers in an octahedral environment with the Pt−Pt bond perpendicular to the equatorial plane, while our dinuclear derivatives display coplanar or nearly coplanar platinum or palladium square-planar coordination environments with the Pt−M (M = Pt, Pd) bond and all Pt or M ligands located in the same plane. As far as we know, complex **5** is the first heteronuclear palladium(III) derivative.

Finally, it is also important to note that usually the oxidative addition of X_2 (X = halogen) to mononuclear Pd(II) and Pt(II) complexes affords halo-M(IV) complexes[33−39] through a 2e oxidation process. Nevertheless the oxidative addition of I_2 to our dinuclear (anionic[18] and neutral) phosphido derivatives of platinum and palladium(II) complexes seems to be a rational way to synthesize platinum(III) and palladium(III) derivatives.

Reduction Reactions of 4 and 5. The addition of NBu_4BH_4 to a solution of **4** (2:1 molar ratio) allows the isolation of the platinum(II) tetranuclear derivative $[NBu_4]_2[(C_6F_5)_2Pt(\mu\text{-}PPh_2)_2Pt(\mu\text{-I})_2Pt(\mu\text{-}PPh_2)_2Pt(C_6F_5)_2]$, **6**, as a yellow solid (Scheme 1). All spectroscopic features of **6** are given in the Experimental Section, and they are similar to those observed for the analogous $[NBu_4]_2[(C_6F_5)_2Pt(\mu\text{-}PPh_2)_2Pt(\mu\text{-X})_2Pt(\mu\text{-}PPh_2)_2Pt(C_6F_5)_2]$ (X = Cl,[19] Br[40]). The reaction that gives **6** can be understood as a two-electron reduction of **4** to give the anionic platinum(II) $[(C_6F_5)_2Pt(\mu\text{-}PPh_2)_2PtI_2]^{2-}$, which after spontaneous elimination of an iodide anion causes the dimerization and isolation of **6** as a solid (Scheme 1). This dimerization process has been observed frequently.[19,41]

When NBu_4BH_4 is added to the heteronuclear complex **5**, under conditions similar to those for **4**, instantaneously the solution turns very dark in color. The IR and NMR spectra of the black solid obtained led us to identify the platinum(II)−palladium(II) complex $[NBu_4]_2[(C_6F_5)_2Pt(\mu\text{-}PPh_2)_2Pd(\mu\text{-I})_2Pd(\mu\text{-}PPh_2)_2Pt(C_6F_5)_2]$, **7**, by comparing with an authentic sample prepared by reacting the chloro derivative $[NBu_4]_2[(C_6F_5)_2Pt(\mu\text{-}PPh_2)_2Pd(\mu\text{-Cl})_2Pd(\mu\text{-}PPh_2)_2Pt(C_6F_5)_2]$[19] with KI (see Experimental Section). In addition other signals due to unidentified products are observed.

Reductive Coupling of PPh_2 and C_6F_5 from M(III) Complexes. When a CH_2Cl_2 solution of **4** or **5** is stirred at room temperature for a long time (see Experimental Section), the tetranuclear M(II) complexes $[\{(C_6F_5)M(\mu\text{-}PPh_2)(\mu\text{-I})M'(PPh_2C_6F_5)(\mu\text{-I})\}_2]$ (M = M′ = Pt, **8**; M = Pt, M′ = Pd, **9**) crystallize as a yellow or brown solid, respectively. As we have commented above, the dinuclear palladium(III) derivative cannot be isolated from the addition of I_2 to complex **3**, but the tetranuclear complex $[\{(C_6F_5)Pd(\mu\text{-}PPh_2)(\mu\text{-I})Pd(PPh_2C_6F_5)(\mu\text{-I})\}_2]$, **10**, analogous to **8** and **9**, is obtained even working at

(29) Lippert, B. *Coord. Chem. Rev.* **1999**, 263−295.
(30) Muller, J.; Freisinger, E.; Sanz-Miguel, P. J.; Lippert, B. *Inorg. Chem.* **2003**, *42*, 5117−5125.
(31) Cotton, F. A.; Gu, J.; Murillo, C. A.; Timmons, D. J. *J. Am. Chem. Soc.* **1998**, *120*, 13280−13281.
(32) Berry, J. F.; Cotton, F. A.; Ibragimov, S. A.; Murillo, C. A.; Wang, J. C. *Inorg. Chem.* **2005**, *44*, 6129−6137.
(33) Ruiz, J.; López, J. F. J.; Rodríguez, V.; Pérez, J.; Ramírez de Arellano, M. C.; López, G. *J. Chem. Soc., Dalton Trans.* **2001**, 2683−2689.
(34) Gossage, R. A.; Ryabov, A. D.; Spek, A. L.; Stufkens, D. J.; van Beek, J. A. M.; van Eldik, R.; van Koten, G. *J. Am. Chem. Soc.* **1999**, *121*, 2488−2497.
(35) Forniés, J.; Menjón, B.; Sanz-Carillo, M. R.; Tomás, M.; Connelly, N. G.; Crossley, J. G.; Orpen, A. G. *J. Am. Chem. Soc.* **1995**, *117*, 4295−4304.
(36) Forniés, J.; Fortuño, C.; Gómez, M. A.; Menjón, B. *Organometallics* **1993**, *12*, 4368−4375.
(37) Usón, R.; Forniés, J.; Tomás, M.; Menjón, B.; Bau, R.; Sünkel, K.; Kuwabara, E. *Organometallics* **1986**, *5*, 1576−1581.
(38) Gracia, C.; Marco, G.; Navarro, R.; Romero, P.; Soler, T.; Urriolabeitia, E. P. *Organometallics* **2003**, *22*, 4910−4921.
(39) van Belzen, R.; Elsevier, C. J.; Dedieu, A.; Veldman, N.; Spek, A. L. *Organometallics* **2003**, *22*, 722−736.
(40) Forniés, J.; Fortuño, C.; Gil, R.; Martín, A. *Inorg. Chem.* **2005**, *44*, 9534−9541.
(41) Usón, R.; Forniés, J.; Tomás, M.; Fandos, R. *J. Organomet. Chem.* **1984**, *263*, 253−260.

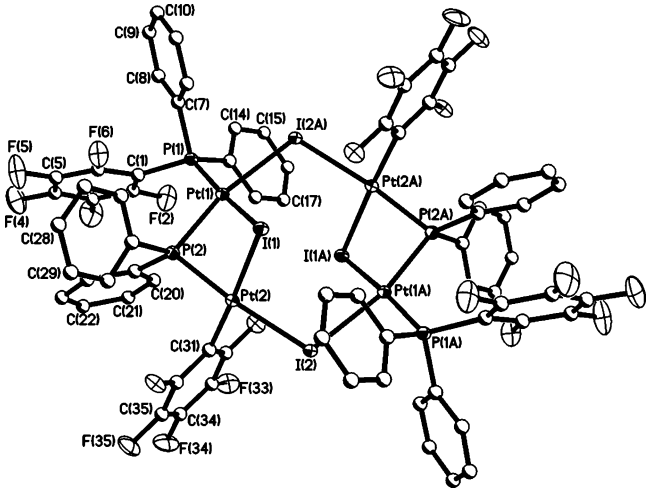

Figure 2. Structure of complex $[\{(C_6F_5)Pt(\mu\text{-}PPh_2)(\mu\text{-}I)Pt(PPh_2C_6F_5)(\mu\text{-}I)\}_2]$ (**8**).

Table 2. Bond Lengths (Å) and Angles (deg) for $[\{(C_6F_5)Pt(\mu\text{-}PPh_2)(\mu\text{-}I)Pt(PPh_2C_6F_5)(\mu\text{-}I)\}_2]\cdot 4CH_2Cl_2$[a]

Pt(1)−P(1)	2.2019(16)
Pt(1)−P(2)	2.2989(16)
Pt(1)−I(1)	2.6223(5)
Pt(1)−I(2)#1	2.7556(5)
Pt(1)−Pt(2)	3.2286(4)
Pt(2)−C(31)	1.962(6)
Pt(2)−P(2)	2.2497(16)
Pt(2)−I(1)	2.5861(5)
Pt(2)−I(2)	2.6975(4)
I(2)−Pt(1)#1	2.7556(5)
P(1)−Pt(1)−P(2)	104.73(6)
P(1)−Pt(1)−I(1)	172.49(4)
P(2)−Pt(1)−I(1)	78.69(4)
P(1)−Pt(1)−I(2)#1	87.03(4)
P(2)−Pt(1)−I(2)#1	166.96(4)
I(1)−Pt(1)−I(2)#1	90.321(14)
C(31)−Pt(2)−P(2)	96.54(18)
C(31)−Pt(2)−I(1)	176.69(17)
P(2)−Pt(2)−I(1)	80.35(4)
C(31)−Pt(2)−I(2)	87.84(17)
P(2)−Pt(2)−I(2)	174.18(4)
I(1)−Pt(2)−I(2)	95.198(14)

[a] Symmetry transformations used to generate equivalent atoms: #1 $-x+2, -y+1, -z+1$.

low temperature. Only complex **8** is soluble enough in the usual organic solvents to grow crystals adequate for X-ray purposes, and the structure of $[\{(C_6F_5)Pt(\mu\text{-}PPh_2)(\mu\text{-}I)Pt(PPh_2C_6F_5)(\mu\text{-}I)\}_2]\cdot 4CH_2Cl_2$ has been analyzed by X-ray diffraction. Figure 2 shows the structure of the complex, and selected bond distances and angles are collected in Table 2.

This complex is a tetrametallic unit that can be regarded as formed by two noncoplanar dinuclear moieties "$\{(C_6F_5)Pt(\mu\text{-}PPh_2)(\mu\text{-}I)Pt(PPh_2C_6F_5)$" held together by two bridging I ligands. The halves of the molecule are related by an inversion center. Each platinum atom lies in a square-planar environment formed by two mutually cis iodide groups, a PPh_2 ligand, and, finally, a $PPh_2C_6F_5$ ligand or a C_6F_5 group in the case of Pt(1) or Pt(2), respectively. The PPh_2 and I(1) are bridging both platinum atoms, while I(2) links the two Pt_2 subunits of the molecule. The angles around Pt(1) range from 78.69(4)° to 104.73(6)°, while for Pt(2) they range from 80.35(4)° to 96.54(18)°, showing a greater distortion of the environment in the case of Pt(1). The dihedral angle formed by the coordination planes of both platinum atoms is 62.3°. The four platinum atoms P(2), P(2A), I(2), and I(2A) form an almost perfect plane, and the C_6F_5 rings

Table 3. Crystal Data and Structure Refinement for $4\cdot 2CHCl_3$ and $8\cdot 4CH_2Cl_2$

	$4\cdot 2CHCl_3$	$8\cdot 4CH_2Cl_2$
empirical formula	$C_{38}H_{22}Cl_6F_{10}I_2P_2Pt_2$	$C_{76}H_{48}Cl_8F_{20}I_4P_4Pt_4$
fw	1587.18	3036.58
temp, K	100(2)	100(2)
wavelength, Å	0.71073	0.71073
cryst syst	triclinic	triclinic
space group	$P\bar{1}$	$P\bar{1}$
a, Å	9.2917(12)	11.0208(7)
b, Å	14.3188(18)	11.7041(7)
c, Å	17.576(2)	17.0947(6)
α, deg	85.143(2)	76.621(1)
β, deg	80.584(2)	78.267(1)
γ, deg	74.207(2)	81.452(1)
volume, Å^3	2217.9(5)	2088.4(2)
Z	2	1
calcd density, Mg/m^3	2.377	2.414
abs coeff, mm^{-1}	8.198	8.577
F(000)	1468	1404
cryst size, mm	0.24 × 0.16 × 0.12	0.27 × 0.20 × 0.13
θ range for data collecn, deg	1.48 to 23.27	1.80 to 29.74
limiting indices	*h*, ± 10; *k*, ± 15; *l*, ± 19	*h*, ± 14; *k*, ± 15; *l*, ± 22
no. of reflns collected/unique	14 429/6362 [*R*(int) = 0.0196]	19 773/9686 [*R*(int) = 0.0345]
refinement method	full-matrix least-squares on F^2	full-matrix least-squares on F^2
no. of data/ restraints/params	6362/0/541	9686/0/523
goodness-of-fit on F^2 [a]	1.015	0.941
final *R* indices [$I>2\sigma(I)$][b]	R1 = 0.0205, wR2 = 0.0417	R1 = 0.0343, wR2 = 0.0705
R indices (all data)[b]	R1 = 0.0231, wR2 = 0.0424	R1 = 0.0447, wR2 = 0.0727
largest diff peak/hole, e Å^{-3}	0.795 and −0.770	1.992 and −1.501

[a] Goodness-of-fit = $[\sum w(F_o^2 - F_c^2)^2/(n_{obs} - n_{param})]^{1/2}$. [b] $R1 = \sum(|F_o| - |F_c|)/\sum|F_o|$; $wR2 = [\sum w(F_o^2 - F_c^2)^2/\sum w(F_c^2)^2]^{1/2}$. $w = [\sigma^2(F_o) + (g_1P)^2 + g_2P]^{-1}$; $P = [\max(F_o^2; 0) + 2F_c^2]/3$.

form a dihedral angle with this plane of 100.8°. The shortest Pt−Pt distance is 3.299 Å, excluding any kind of metal−metal interaction.

The poor solubility of the complexes in common organic solvents precludes obtention of NMR data for all but complex **8**. The ^{19}F NMR spectrum of **8** shows three signals (2:1:2 intensity ratio) due to *o*-F, *p*-F, and *m*-F atoms of the $PPh_2C_6F_5$ ligand[18,42−45] and five signals due to the five unequivalent atoms of the C_6F_5 bonded to the platinum center. These signals are broad and of low intensity, and although platinum satellites are perceptible, the coupling values between *o*-F and Pt atoms cannot be calculated accurately. Nevertheless, the number of signals as well as their pattern indicated that the two organometallic C_6F_5 groups are equivalent and that the two *o*-F atoms, as well as the two *m*-F ones, within each ring are unequivalent, in agreement with the solid-state structure. This inequivalence within each organometallic C_6F_5 group indicates that the pentafluorophenyl ring is not free to rotate around the Pt−C_{ipso} bond in this nonplanar molecule. In the ^{31}P NMR spectrum two signals at −1.0 and −59.7 ppm due to the phosphine and phosphido ligands, respectively, are observed. The chemical shift due to the P atom of the phosphido group appears at higher

(42) Ara, I.; Forniés, J.; García, A.; Gómez, J.; Lalinde, E.; Moreno, M. T. *Chem. Eur. J.* **2002**, *8*, 3698−3716.
(43) Falvello, L. R.; Forniés, J.; Fortuño, C.; Martín, A.; Martínez-Sariñena, A. P. *Organometallics* **1997**, *16*, 5849−5856.
(44) Usón, R.; Forniés, J.; Espinet, P.; Lalinde, E.; Jones, P. G.; Sheldrick, G. M. *J. Chem. Soc., Dalton Trans.* **1982**, 2389−2395.
(45) Usón, R.; Forniés, J.; Espinet, P.; Lalinde, E. *J. Organomet. Chem.* **1983**, *254*, 371−379.

field than for the starting material **4** (280.5 ppm), in agreement with the long intermetallic distance in **8**, 3.2286(4) Å, and at lower field than for complexes that show the "Pt(μ-PPh_2)$_2$Pt" system without a metal−metal bond. This value (−59.7 ppm) is similar to those observed for other "M(μ-PPh_2)(μ-X)M" (X = Cl, Br, I, OH) frameworks without metal−metal bonds.[7,18,40,46]

The IR spectra of **8**−**10** are almost superimposable, pointing to an analogous structure for all complexes. In the three cases an absorption at ca. 1520 cm^{-1} and another at ca. 980 cm^{-1} are indicative of the presence of the $PPh_2C_6F_5$ ligand.[18,43] In addition, in the 800 cm^{-1} region only one absorption is observed, in agreement with the presence of only a C_6F_5 group bonded to the metal center,[26,27] while two absorptions are present for the starting material in which two C_6F_5 groups are bonded to the same metal center in a cis geometry. Complex **9** contains two platinum and two palladium centers, and, as in **8** and **10**, only one absorption is observed for the C_6F_5 group in the X-sensitive region. The wavenumber of this signal appears at 804 cm^{-1} (15 cm^{-1} higher than for the palladium complex **10**), in agreement with a structure in which the C_6F_5 groups are bonded to the platinum centers;[17,19,47] thus the two $PPh_2C_6F_5$ ligands have to be bonded to the palladium centers. This information allowed a tentative assignment of the structure of **9** as depicted in Scheme 1.

The formation of **8** and **9** from **4** and **5**, respectively, are new examples of the very rare reductive coupling process between a PPh_2 and a C_6F_5 anion bonded to M, which yields the tertiary phosphine $PPh_2C_6F_5$ (Scheme 1). This process seems to indicate that the unusually planar dinuclear M(III) derivatives **4** and **5** (30 valence electron count, one metal−metal bond) are not stable enough and that the formation of the M(II) derivatives is preferred even by using for reduction this unusual reductive coupling.

The reaction of complex **3** with I_2, which results in the formation of **10**, can be easily understood by considering that in the intermediate palladium(III) [$(C_6F_5)_2$Pd(μ-PPh_2)$_2$Pd$(C_6F_5)_2$] derivative (if formed) the Pd−C_6F_5 and Pd−PPh_2 bonds should be much more labile, this fact favoring the reductive coupling and avoiding detection of this Pd(III) intermediate.

Finally, a great number of synthetic procedures and catalytic processes in platinum and palladium chemistry are understood by oxidative addition−reductive coupling (with or without elimination) sequences.[39,48−52] The addition to M(0) or M(II) complexes gives M(II) or M(IV) derivatives (M = Pd, Pt), respectively, and a reductive process regenerates new M(0) or M(II) derivatives. Nevertheless the synthesis of the M(II) **8**−**10** from the M(II) **1**−**3** is carried out through platinum or palladium(III) intermediates.

DFT Calculations of the Geometric and Energetic Profile of the Reaction of [$(C_6F_5)_2$M(μ-PH_2)$_2$M′(NCCH$_3$)$_2$] (M = M′ = Pt or Pd, M = Pt, M′ = Pd) Complexes with I_2 in the Gas Phase. To furnish details on the structural and energetic changes that accompany the reaction of the neutral [$(C_6F_5)_2$M-(μ-PH_2)$_2$M′(NCCH$_3$)$_2$] (M = M′ = Pt or Pd, M = Pt, M′ = Pd) complexes with I_2, the potential energy surfaces (PES) of the reactions in the gas phase were computed by DFT methods (at the B3LYP/lanl2dz level). Because of the computational cost due to the relatively big size of the compounds under consideration, to obtain a computationally convenient size, we used models resulting upon substitution of only the phenyl groups of the phosphido ligands by H atoms. Furthermore, the formation of the neutral [$(C_6F_5)_2$M(μ-PH_2)$_2$M′(NCCH$_3$)$_2$] (M = M′ = Pt or Pd, M = Pt, M′ = Pd) complexes upon acidifying acetonitrile solutions of [$(C_6F_5)_2$Pt(μ-PH_2)$_2$Pd$(C_6F_5)_2]^{2-}$ and [$(C_6F_5)_2$Pd(μ-PH_2)$_2$Pd(acac)]$^-$ complexes has also been investigated at the B3LYP/lanl2dz level of theory. An abbreviated report of this computational study is discussed here, while a more detailed account is given as Supporting Information. The equilibrium geometries of the [$(C_6F_5)_2$M(μ-PH_2)$_2$M′(NCCH$_3$)$_2$] (M = M′ = Pt, **M1**; M = Pt, M′ = Pd; **M2**; M = M′ = Pd, **M3**) complexes and the total electronic energies and selected electronic properties of the complexes are given in Figure 4S and Table 4S, respectively (Supporting Information). The salient structural feature of the [$(C_6F_5)_2$M(μ-PH_2)$_2$M′(NCCH$_3$)$_2$] (M = M′ = Pt, **M1**; M = Pt, M′ = Pd; **M2**; M = M′ = Pd, **M3**) complexes is the flexible dihedral angle between the two MP2 planes that describes the degree of folding of the M(μ-PH_2)$_2$M′ ring along the P···P axis.

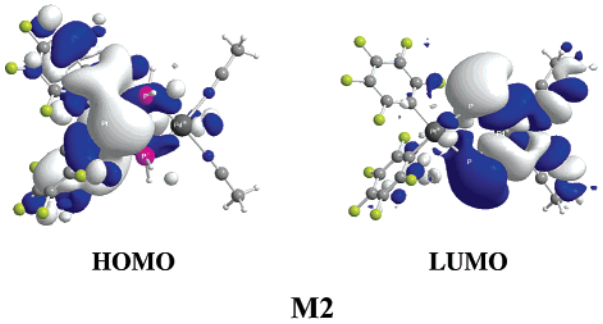

Figure 3. 3-D plots of the HOMO and LUMO of complex **M2**.

The metal centers in **M1** acquire a positive natural atomic charge, which is slightly higher for the Pt center associated with the MeCN ligand. The opposite is true for the metal centers in **M3**, where the Pd center associated with the MeCN ligand acquires a slightly lower positive natural atomic charge (Table 4S). In **M2** the Pd is the metal center acquiring the higher positive natural atomic charge. The N donor atom of the MeCN ligands in all complexes acquires the higher negative natural atomic charge amounting to −0.47 |e|. According to the hardness values, both homonuclear complexes are more stable than the heteronuclear one, with the stability following the trend **M1** > **M3** > **M2**.The 3-D plots of the frontier molecular orbitals (FMOs) directly involved in the oxidative addition of I2 to a representative complex M2 are shown in Figure 3. Analogous are the 3-D plots of the FMOs of **M1** and **M3**. The HOMO of all complexes consists of an antibonding combination of nd_{z^2} orbitals of the two metal centers mainly localized on the metal center coordinated with the C_6F_5 ligands, having also a small contribution from a π MO of the C_6F_5 ligands in an out-of-phase fashion. On the other hand, the LUMO consists of a bonding combination of $nd_{x^2-y^2}$ orbitals of the two metal centers mainly localized on the metal center coordinated with the MeCN ligands and having significant contribution from a σ* MO localized on the CN moiety participating in an antibonding combination mode.

The nature of the FMOs of **M1**, **M2**, and **M3** imply that the HOMO of the I_2 molecule, being a σ MO, could interact with

(46) Alonso, E.; Forniés, J.; Fortuño, C.; Martín, A.; Rosair, G. M.; Welch, A. J. *Inorg. Chem.* **1997**, *36*, 4426−4431.
(47) Usón, R.; Forniés, J.; Tomás, M.; Martínez, F.; Casas, J. M.; Fortuño, C. *Inorg. Chim. Acta* **1995**, *235*, 51−60.
(48) Christmann, U.; Vilar, R. *Angew. Chem., Int. Ed.* **2005**, *44*, 366−374.
(49) Leca, F.; Sauthier, M.; Deborde, V.; Toupet, L.; Réau, R. *Chem. Eur. J.* **2003**, *9*, 3785−3795.
(50) Moncarz, J. R.; Brunker, T. J.; Glueck, D. S.; Sommer, R. D.; Rheingold, A. L. *J. Am. Chem. Soc.* **2003**, *125*, 1180−1181.
(51) Hristov, I. H.; Ziegler, T. *Organometallics* **2003**, *22*, 3513−3525.
(52) Espinet, P.; Echavarren, A. M. *Angew. Chem., Int. Ed.* **2004**, *42*, 4704−4734.

the LUMO of the complexes which is mainly localized on the metal center coordinated with the MeCN ligands. The HOMO−LUMO interaction weakens both the I−I and M−NCMe bonds due to charge transfer from a bonding (HOMO of I_2) to an antibonding orbital with respect to the M−NCMe bond MO of the complex. Moreover, possible interactions of the HOMOs of the complexes with the LUMO (a σ^* MO) of the I_2 molecule could not be excluded. Such interactions contribute further to the weakening of the I−I and M−NCMe bonds and the formation of the final oxidation product $[(C_6F_5)_2M(\mu\text{-}PH_2)_2M'I_2]$ (M = M′ = Pt, **M4**; M = Pt, M′ = Pd **M5** (see Figure 5S, Supporting Information).

Equilibrium Geometry, Electronic Structure, and Bonding Mechanism in the $[(C_6F_5)_2M(\mu\text{-}PH_2)_2M'I_2]$ (M = Pt, M′ = Pd; M = M′ = Pt or Pd) Complexes. The equilibrium geometries of the $[(C_6F_5)_2M(\mu\text{-}PH_2)_2M'I_2]$ (M = M′ = Pt, **M4**; M = Pt, M′ = Pd; **M5**; M = M′ = Pd, **M6**) complexes, the total electronic energies, and some electronic properties of the complexes computed at the B3LYP/lanl2dz level of theory are given in Figure 5S and Table 5S, respectively (Supporting Information). Overall, the B3LYP/lanl2dz calculations reproduce very well the experimentally observed structural parameters of $[(C_6F_5)_2Pt(\mu\text{-}PPh_2)_2PtI_2]$, **4**. The most characteristic structural parameter of the complexes related with the reductive coupling of PH_2 and C_6F_5 is the narrowing of the P−Pt−C_{ipso} and P−Pd−C_{ipso} bond angles having the P atom common with the P−M−I bond angle involving the longer M−I bond. This narrowing forces the P donor atom of the bridging phosphido ligand to be closer to the C_{ipso} atom of the C_6F_5 ligand; the P−C_{ipso} separation distances are 2.949, 2.880, and 2.781 Å for **M4**, **M5**, and **M6**, respectively. The P−C_{ipso} separation distances being shorter than the sum of the van der Waals radii of the P and C atoms (3.246 Å) indicate the existence of weak P···C_{ipso} interactions, which can promote the reductive coupling of PH_2 and C_6F_5. It is evident that the shorter P···C_{ipso} separation distance in the dipalladium complex **M6** corresponds to much stronger P···C_{ipso} interactions, which account well for our unsuccessful attempts to isolate the $[(C_6F_5)_2Pd(\mu\text{-}PPh_2)_2PdI_2]$ complex. Obviously, the $[(C_6F_5)_2Pd(\mu\text{-}PPh_2)_2PdI_2]$ complex immediately rearranges to the tetranuclear complex **10**, through the reductive coupling of PPh_2 and C_6F_5. It should be noted that according to the total electronic energies and the hardness values (Table 5S, Supporting Information) the stability of the complexes follows the trend **M6** > **M5** > **M4**, which means that the dipalladium complex is thermodynamically more stable; thereby one would expect **M6** to be isolated from the reaction mixture as is the case for **M4** and **M5**. However, it is the kinetic instability of **M6** toward the reductive coupling process responsible for **M6** being a transient species that could not be isolated. Both metal centers in **M4**, **M5**, and **M6** acquire a positive natural atomic charge, which is lower in the metal center coordinated with the iodide ligands. The iodide ligands acquire negative natural atomic charge, with that more strongly coordinated with the metal center bearing much higher negative natural atomic charge (Table 5S, Supporting Information). The two-electron (2e) reduction of **M4** and **M5** enforces the dissociation of one of the iodide ligands, yielding **M7** and **M8**, respectively (Scheme 4S, Supporting Information). The overall process is predicted to be exothermic, with exothermicities of 154 and 147 kcal/mol, respectively, at the B3LYP/lanl2dz level.

To understand the dissociation of one of the iodide ligands upon 2e reduction of **M4** and **M5**, we looked at the acceptor orbital (the LUMO) of the complexes. The 3-D plots of the HOMO and LUMO of a representative complex **M5** are shown in Figure 4. Analogous are the 3-D plots of the HOMO and LUMO of **M4** and **M6**. It can be seen that the LUMOs of **M4**, **M5**, and **M6** correspond to Pt−P and Pd−P bonding molecular orbitals localized mainly on the Pt(μ-P)$_2$Pt, Pt(μ-P)$_2$Pd, and Pd(μ-P)$_2$Pd "rhombus", respectively, with significant contribution from Pt−I and Pd−I antibonding interactions related with the weaker Pt−I and Pd−I bonds. Therefore, the 2e reduction of the complexes accumulates electron density on the Pt−I or Pd−I antibonding LUMOs, thus enforcing the dissociation of the respective bonds and the formation of the monomeric species **M7** and **M8** (Scheme 4S). The nature of the FMOs of **M7** and **M8** complexes (Figure 5) accounts well for their easy dimerization, which is supported by favorable HOMO−LUMO interactions.

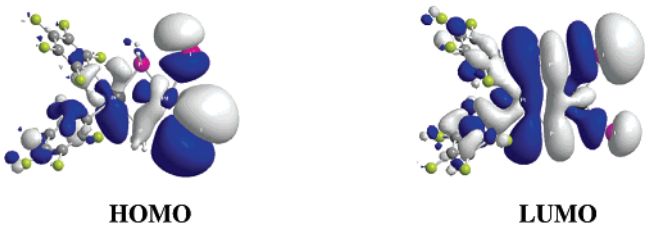

M5

Figure 4. 3-D plots of the HOMO and LUMO of complex **M5**.

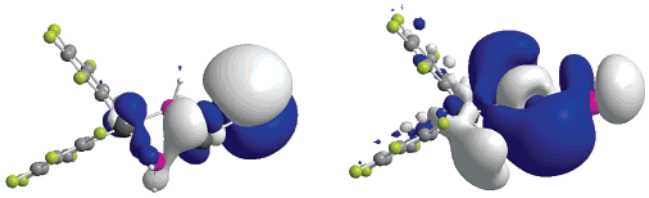

M8

Figure 5. 3-D plots of the HOMO and LUMO of complex **M8**.

Thus, one molecule could act as a ligand through its donor orbital (HOMO) exhibiting high 5p(I) orbital character interacting with the acceptor orbital (LUMO) exhibiting high nd(M) character of the other molecule, resulting in the formation of two M−I−M bridges. Along this line the formation of the dimeric species **6** and **7** can be easily understood.

Concluding Remarks

The binuclear neutral M(II) derivatives $[(C_6F_5)_2M(\mu\text{-}PPh_2)_2M'(NCCH_3)_2]$ (M = M′ = Pt, **1**; M = Pt, M′ = Pd, **2**) are oxidized with I_2, yielding the corresponding binuclear M(III) derivatives $[(C_6F_5)_2M(\mu\text{-}PPh_2)_2M'I_2]$ (M = M′ = Pt, **4**; M = Pt, M′ = Pd, **5**). The oxidation reaction is accompanied by a substitution process so that the iodo complexes are formed. The M(III) complexes **4** and **5** are stable in the solid state, but in solution they show a clear tendency to reduction. In the presence of a reducing reagent such as $[NBu_4][BH_4]$ the corresponding M(II) derivatives $[NBu_4]_2[(C_6F_5)_2M(\mu\text{-}PPh_2)_2M'(\mu\text{-}I)_2M'(\mu\text{-}PPh_2)_2M'(C_6F_5)_2]$ (M = M′ = Pt, **6**; M = Pt, M′ = Pd, **7**) are formed. In the absence of a reducing agent, an intramolecular reductive coupling of PPh_2 and C_6F_5 takes place to form $PPh_2C_6F_5$ and M(II) derivatives $[\{(C_6F_5)M(\mu\text{-}PPh_2)(\mu\text{-}I)M'(PPh_2C_6F_5)(\mu\text{-}I)\}_2]$ (M = M′ = Pt, **8**; M = Pt, M′ = Pd, **9**). For the binuclear homometallic palladium compound $[(C_6F_5)_2Pd(\mu\text{-}PPh_2)_2Pd(NCCH_3)_2]$, **3**, the reaction with I_2 does not allow the isolation of the Pd(III)−Pd(III) derivative but only the complex resulting from the reductive coupling, $[\{(C_6F_5)Pd(\mu\text{-}PPh_2)(\mu\text{-}I)Pd$-

$(PPh_2C_6F_5)(\mu\text{-}I)\}_2]$, **10**, in keeping with the higher lability of the palladium derivatives.

It is also noteworthy that although reduction to M(II) complexes could also occur through the coupling of the PPh_2 and I groups (formation of PPh_2I), no evidence of such a process has been obtained. In these complexes the formation of a P−C bond is preferred to the formation of a P−I one.

The structural, bonding, electronic, and related properties of all compounds studied herein have been satisfactory described by DFT computational techniques at the B3LYP/lanl2dz level of theory. The chemical behavior of the $[(C_6F_5)_2M(\mu\text{-}PH_2)_2M'(NCCH_3)_2]$ (M = M′ = Pt or Pd, M = Pt, M′ = Pd) complexes toward their reaction with I_2 was also explained in the framework of the qualitative frontier molecular orbital theory.

Experimental Section

General Procedures and Materials. C, H, and N analyses were performed with a Perkin-Elmer 240B microanalizer. IR spectra were recorded on a Perkin-Elmer Spectrum One spectrophotometer (Nujol mulls between polyethylene plates in the range 4000−350 cm^{-1}). NMR spectra were recorded on a Varian Unity 300 instrument with $SiMe_4$, $CFCl_3$, and 85% H_3PO_4 as external references for ^1H, ^{19}F, and ^{31}P, respectively. Conductivities (acetone $c \approx 5 \times 10^{-4}$ M) were measured with a Philips PW 9509 conductimeter. Literature methods were used to prepare the starting complexes $[(C_6F_5)_2Pt(\mu\text{-}PPh_2)_2Pt(NCCH_3)_2]$,[21] $[NBu_4]_2[(C_6F_5)_2Pt(\mu\text{-}PPh_2)_2Pd(C_6F_5)_2]$,[19] and $[NBu_4][(C_6F_5)_2Pd(\mu\text{-}PPh_2)_2Pd(acac)]$.[20]

Safety Note. Perchlorate salts of metal complexes with organic ligands are potentially explosive. Only small amounts of materials should be prepared, and these should be handled with great caution.

Synthesis of $[(C_6F_5)_2Pt(\mu\text{-}PPh_2)_2Pd(NCCH_3)_2]$ (2). To a yellow solution of $[NBu_4]_2[(C_6F_5)_2Pt(\mu\text{-}PPh_2)_2Pd(C_6F_5)_2]$ (0.300 g, 0.164 mmol) in acetonitrile (15 mL) was added $HClO_4$ (0.327 mmol, MeOH solution), and a yellow solid, **6**, starts to crystallize. After 1.5 h stirring at room temperature the mixture was evaporated to 3 mL, and ^{i}PrOH (3 mL) was added. **6** was collected by filtration and washed with 2 × 0.5 mL of ^{i}PrOH (0.135 g, 76% yield). Anal. Found (calcd for $C_{40}F_{10}H_{26}N_2P_2PtPd$): C, 44.6 (44.8); H, 2.1 (2.4); N, 2.45 (2.6). IR (Nujol, cm^{-1}): 786 and 774 (X-sensitive C_6F_5 group);[26,27] 2313, 2286 ($\nu_N{\equiv}C$).[53] ^{19}F NMR (293 K, deuteroacetone, 282.4 MHz, δ): −114.6 (4 *o*-F, $^3J_{Pt,F}$ = 327 Hz), −162.4 (6 *m*- + *p*-F) ppm. $^{31}P\{^1H\}$ NMR (293 K, deuteroacetone, 121.5 MHz, δ): −130.4 ($^1J_{Pt,P}$ = 1785 Hz) ppm.

Synthesis of $[(C_6F_5)_2Pd(\mu\text{-}PPh_2)_2Pd(NCCH_3)_2]$ (3). To a yellow solution of $[NBu_4][(C_6F_5)_2Pd(\mu\text{-}PPh_2)_2Pd(acac)]$ (0.440 g, 0.350 mmol) in acetonitrile (5 mL) was added $HClO_4$ (0.350 mmol, MeOH solution). After 30 min stirring the mixture was evaporated to ca. 2 mL and ^{i}PrOH (3 mL) was added. A yellow solid, **6**, crystallized, which was collected by filtration and washed with 0.5 mL of ^{i}PrOH (0.262 g, 75% yield). Anal. Found (calcd for $C_{40}F_{10}H_{26}N_2P_2Pd_2$): C, 47.8 (48.1); H, 2.4 (2.6); N, 2.8 (2.8). IR (Nujol, cm^{-1}): 773 and 763 (X-sensitive C_6F_5 group); 2317, 2290 ($\nu_N{\equiv}C$). ^{19}F NMR (293 K, deuteroacetone, 282.4 MHz, δ): −111.5 (4 *o*-F), −164.6 (2 *p*-F), −164.9 (4 *m*-F) ppm. $^{31}P\{^1H\}$ NMR (293 K, deuteroacetone, 121.5 MHz, δ): −106.0 ppm.

Synthesis of $[(C_6F_5)_2Pt(\mu\text{-}PPh_2)_2MI_2]$ (M = Pt 4, Pd 5). M = Pt. To a white suspension of **1** (0.200 g, 0.170 mmol) in CH_2Cl_2 (5 mL)/acetonitrile (8 mL) at 213 K was added an acetonitrile solution (8 mL) of I_2 (0.046 g, 0.181 mmol). The color of the suspension turned red, and after 20 min stirring at 213 K the mixture was evaporated to 5 mL. The dark red solid, **4**, was filtered off and washed with 0.5 mL of cold ^{i}PrOH (0.179 g, 78% yield). Anal. Found (calcd for $C_{36}F_{10}H_{20}I_2P_2Pt_2$): C, 32.0 (32.1); H, 1.3 (1.5). IR (Nujol, cm^{-1}): 791 and 779 (X-sensitive C_6F_5 group). ^{19}F NMR (293 K, $CDCl_3$, 282.4 MHz, δ): −119.5 (4 *o*-F, $^3J_{Pt,F}$ = 300 Hz), −157.7 (2 *p*-F), −162.0 (4 *m*-F) ppm. $^{31}P\{^1H\}$ NMR (293 K, $CDCl_3$, 121.5 MHz, δ): 280.5 ($^1J_{Pt1,P}$ = 1135, $^1J_{Pt2,P}$ = 1716 Hz) ppm.

M = Pd, 5. To a yellow suspension of **2** (0.110 g, 0.101 mmol) in CH_2Cl_2 (6 mL) at 195 K was added a CH_2Cl_2 solution (5 mL) of I_2 (0.025 g, 0.101 mmol). After 5 min stirring at 195 K the dark brown solution was evaporated to 1 mL and a brown solid start to crystallize. Hexane (4 mL) was added, and the solid **5** was filtered off and washed with 1 mL of hexane (0.070 g, 55% yield). Anal. Found (calcd for $C_{36}F_{10}H_{20}I_2P_2PtPd$): C, 34.0 (34.3); H, 1.5 (1.6). IR (Nujol, cm^{-1}): 795 and 784 (X-sensitive C_6F_5 group). ^{19}F NMR (213 K, CD_2Cl_2, 282.4 MHz, δ): −119.1 (4 *o*-F, $^3J_{Pt,F}$ = 295 Hz), −157.3 (2 *p*-F), −161.5 (4 *m*-F) ppm. $^{31}P\{^1H\}$ NMR (213 K, CD_2Cl_2, 121.5 MHz, δ): 321.5 ($^1J_{Pt,P}$ = 1273 Hz) ppm.

Reduction of $[(C_6F_5)_2Pt(\mu\text{-}PPh_2)_2MI_2]$ (M = Pt 4, Pd 5). M = Pt. To a red solution of **4** (0.100 g, 0.074 mmol) in CH_2Cl_2 (8 mL) was added a CH_2Cl_2 solution (1 mL) of NBu_4BH_4 (0.040 g, 0.155 mmol). The yellow solution was stirred for 3 h, then evaporated to 1 mL. ^{i}PrOH (4 mL) was added, and after 15 min stirring a yellow solid, **6**, was filtered off and washed with 2 × 0.5 mL of ^{i}PrOH (0.076 g, 70% yield). Anal. Found (calcd for $C_{104}F_{20}H_{112}I_2P_4Pt_4$): C, 42.8 (42.7); H, 4.0 (3.85); N, 1.2 (0.95). Λ_M = 186 ohm^{-1} cm^2 mol^{-1}. IR (Nujol, cm^{-1}): 782 and 773 (X-sensitive C_6F_5 group). ^{19}F NMR (213 K, deuteroacetone, 282.4 MHz, δ): −114.0 (8 *o*-F, $^3J_{Pt,F}$ = 320 Hz), −166.2 (8 *m*-F), −167.2 (4 *p*-F) ppm. $^{31}P\{^1H\}$ NMR (213 K, deuteroacetone, 121.5 MHz, δ): −142.3 ($^1J_{Pt,P}$ = 1897 and 2447 Hz) ppm.

M = Pd, 5. The same procedure used for reduction of **4** from **5** (0.100 g, 0.079 mmol) and NBu_4BH_4 (0.045 g, 0.174 mmol) gives a black solid, from which complex **7** is identified by spectroscopy.

Synthesis of $[NBu_4]_2[\{(C_6F_5)Pt(\mu\text{-}PPh_2)_2Pd(\mu\text{-}I)\}_2]$, 7. To a yellow solution of $[NBu_4]_2[\{(C_6F_5)Pt(\mu\text{-}PPh_2)_2Pd(\mu\text{-}Cl)\}_2]$ (0.160 g, 0.062 mmol) in acetone (20 mL) was added KI (0.096 g, 0.578 mmol). The mixture was stirred at room temperature for 20 h and evaporated to dryness. The solid was extracted with CH_2Cl_2 (20 mL), and the solution was evaporated to ca. 1 mL. ^{i}PrOH (10 mL) was added, and after 3 h stirring an orange solid, **7**, was filtered off and washed with 3 × 0.5 mL of ^{i}PrOH (0.109 g, 64% yield). Anal. Found (calcd for $C_{104}F_{20}H_{112}I_2P_4Pt_2Pd_2$): C, 45.5 (45.4); H, 4.25 (4.1); N, 1.0 (1.0). Λ_M = 181 ohm^{-1} cm^2 mol^{-1}. IR (Nujol, cm^{-1}): 785 and 780 (X-sensitive C_6F_5 group). ^{19}F NMR (213 K, deuteroacetone, 282.4 MHz, δ): −113.6 (8 *o*-F, $^3J_{Pt,F}$ = 327 Hz), −166.2 (8 *m*-F), −167.2 (4 *p*-F) ppm. $^{31}P\{^1H\}$ NMR (213 K, deuteroacetone, 121.5 MHz, δ): −131.4 ($^1J_{Pt,P}$ = 1733 Hz) ppm.

Synthesis of $[\{(C_6F_5)M(\mu\text{-}PPh_2)(\mu\text{-}I)M'(PPh_2C_6F_5)(\mu\text{-}I)\}_2]$ (M = M′ = Pt, 8; M = Pt, M′ = Pd, 9; M = M′ = Pd, 10). M = M′ = Pt, 8. A red CH_2Cl_2 solution (15 mL) of **4** (0.150 g, 0.111 mmol) was stirred at room temperature for 60 h. The resulting yellow solution was evaporated to 1 mL, and **8** crystallized as a yellow solid. Hexane (4 mL) was added, and the solid was filtered off (0.099 g, 66% yield). Anal. Found (calcd for $C_{72}F_{20}H_{40}I_4P_4Pt_4$): C, 32.4 (32.1); H, 1.3 (1.5). IR (Nujol, cm^{-1}): 1522 and 983 ($PPh_2C_6F_5$); 799 (X-sensitive C_6F_5 group). ^{19}F NMR (293 K, CD_2Cl_2, 282.4 MHz, δ): −112.9 (2 *o*-F), −119.0 (2 *o*-F), −124.2 (2 *o*-F, $PPh_2C_6F_5$), −147.9 (2 *p*-F, $PPh_2C_6F_5$), −160.2 (4 *m*-F, $PPh_2C_6F_5$), −164.3 (2 *p*-F), −165.2 (2 *m*-F), −166.4 (2 *m*-F) ppm. $^{31}P\{^1H\}$ NMR (213 K, $CDCl_3$, 121.5 MHz, δ): −1.0 ($PPh_2C_6F_5$, $^1J_{Pt,P}$ = 4684 Hz), −59.7 (PPh_2, $^1J_{Pt,P}$ = 2592 and 3287 Hz) ppm.

M = Pt, M′ = Pd, 9. Complex **9** was prepared in the same way as for **5** (0.100 g, 0.079 mmol) with 15 h stirring at room temperature. **9** was formed as a brown solid (0.070 g, 70% yield). Anal. Found (calcd for $C_{72}F_{20}H_{40}I_4P_4Pd_2Pt_2$): C, 34.2 (34.3); H, 1.9 (1.6). IR (Nujol, cm^{-1}): 1520 and 983 ($PPh_2C_6F_5$); 804 (X-sensitive C_6F_5 group).

(53) Murahashi, T.; Nagai, T.; Okuno, T.; Matsutani, T.; Kurosawa, H. *Chem. Commun.* **2000**, 1689−1690.

M = M′ = Pd, 10. To a CH_2Cl_2 solution (8 mL) of I_2 (0.051 g, 0.200 mmol) at 195 K was added **3** (0.200 g, 0.200 mmol), and the dark red solution was stirred for 3 min. The solution was evaporated to 1 mL, and hexane (4 mL) was added. Complex **10** crystallized as a red-brown solid (0.163 g, 70% yield). Anal. Found (calcd for $C_{72}F_{20}H_{40}I_4P_4Pd_4$): C, 36.95 (37.0); H, 1.5 (1.7). IR (Nujol, cm^{-1}): 1521 and 983 ($PPh_2C_6F_5$); 789 (X-sensitive C_6F_5 group).

Crystal Structure Determination. Crystals suitable for X-ray diffraction of the complexes were obtained by slow diffusion of *n*-hexane into solutions of 0.020 g of **4** in chloroforme (3 mL) and a saturated solution of **8** in dichloromethane (3 mL), at 6 °C.

Crystal data and other details of the structure analysis for the three complexes are presented in Table 3. The crystals were mounted on quartz fibers in a random orientation and held in place with a fluorinated oil. Data collection was performed at 100 K temperature on a Bruker Smart CCD diffractometer using graphite-monocromated Mo Kα radiation ($\lambda = 0.71073$ Å) with a nominal crystal to detector distance of 6.0 cm. A sphere of data was colleted on the basis of three ω-scans runs (starting $\omega = -28°$) at values $\phi = 0$, 120, and 240 with the detector at $2\theta = 28°$. At each of these runs 606 frames were collected at 0.3° intervals and 10 s per frame. The diffaction frames were integrated using the SAINT package[54] and corrected for absorption with SADABS.[55] Lorentz and polarization corrections were applied. The structures were solved by direct methods. All non-hydrogen atoms were assigned anisotropic displacement parameters. H atoms were added at calculated positions with equivalent isotropic displacement parameters set equal to 1.2 times those of the corresponding parent atoms. Two molecules of lattice $CHCl_3$ for complex **4** and four molecules of lattice CH_2Cl_2 for complex **8** were also found and refined with anisotropic displacement parameters. Final difference electron density maps showed some peaks above 1 e $Å^{-3}$ for **8**, but none of them has chemical meaning. The structures were refined using the SHELXL-97 program.[56]

Computational Details. The structural, electronic, and energetic properties of all compounds were computed at Becke's three-parameter hybrid functional[57,58] combined with the Lee−Yang−Parr correlation functional[59] abbreviated as the B3LYP level of theory, using the LANL2DZ basis set[60] that includes Dunning/Huzinaga full DZ on first row atoms and Los Alamos ECPs plus DZ for platinum and palladium atoms. In all computations no constraints were imposed on the geometry. Full geometry optimization was performed for each structure using Schlegel's analytical gradient method,[61] and the attainment of the energy minimum was verified by calculating the vibrational frequencies that result in the absence of imaginary eigenvalues. All the stationary points have been identified for minimum (number of imaginary frequencies NIMAG = 0) or transition states (NIMAG = 1). The natural bond orbital (NBO) population analysis was performed using Weinhold's methodology.[62,63] All calculations were performed using the Gaussian 03 series of programs.[64] Moreover, the qualitative concepts and the graphs derived from the Chem3D program suite[65−66] highlight the basic interactions resulting from the DFT calculations.

Acknowledgment. We thank the Ministerio de Ciencia y Tecnología and Fondos FEDER (Project BQU2002-03997-CO2-02), the Diputación General de Aragón for its financial support, and the Agencia Española de Cooperación Internacional (Ministerio de Asuntos Exteriores) for a grant to N.Ch.

Supporting Information Available: Complete ref 64. Crystallographic data in CIF format. A detailed report on the computational study. Tables S1 and S2 summarizing the Cartesian coordinates and energies of all stationary points, respectively. This information is available free of charge via the Internet at http://pubs.acs.org.

OM0508029

(54) *SAINT* version 5.0; Bruker Analytical X-ray Systems: Madison, WI.

(55) Sheldrick, G. M. *SADABS*, empirical absorption program; University of Gottingen: Germany, 1996.

(56) Sheldrick, G. M. *SHELXL-97*, a program for crystal structure determination; University of Gottingen: Germany, 1997.

(57) Becke, A. D. *J. Chem. Phys.* **1992**, *96*, 215−2160.

(58) Becke, A. D. *J. Chem. Phys.* **1993**, *98*, 5648−5652.

(59) Lee, C. T.; Yang, W. T.; Parr, R. G. *Phys. Rev.* **1988**, *B37*, 785−789.

(60) Wadt, W. R.; Hay, P. J. *J. Chem. Phys.* **1985**, *82*, 284−298.

(61) Schlegel, H. B. *J. Comput. Chem.* **1982**, *3*, 214−218.

(62) Reed, A. E.; Curtiss, L. A.; Weinhold, F. *Chem. Rev.* **1988**, *88*, 899−926.

(63) Weinhold, F. In *The Encyclopedia of Computational Chemistry*; Schleyer, P. v. R., Ed.; John Wiley & Sons: Chichester, 1998; pp 1792−1811.

(64) Frisch, M. J. T.; et-al. *Gaussian 03*, Revision B. 02; Gaussian, Inc.: Pittsburgh, PA, 2003. See Supporting Information for the remaining 80 authors.

(65) *ChemOffice 97*; Cambridge Scientific Computing, I: 875 Massachusetts Ave., Suite 41, Cambridge, MA 02139.

(66) Diez, A.; Forniés, J.; García, A.; Lalinde, E.; Moreno, M. T. *Inorg. Chem. Commun.*, in press, INOCHE-D-05-00339.